



ELSEVIER

Spectrochimica Acta Part B 57 (2002) 843–852

SPECTROCHIMICA  
ACTA  
PART B

www.elsevier.com/locate/sab

# Chemiluminescent emission spectra of lead, chromium, ruthenium, iron, manganese, rhenium, osmium and tungsten in the reactive flow detector

Kevin B. Thurbide<sup>a,\*</sup>, Walter A. Aue<sup>b</sup>

<sup>a</sup>Department of Chemistry, University of Calgary, 2500 University Drive, N.W., Calgary, Alberta, Canada T2N 1N4

<sup>b</sup>Department of Chemistry, Dalhousie University, Halifax, Nova Scotia, Canada B3H 4J3

Received 27 August 2001; accepted 23 January 2002

## Abstract

Spectra have been measured of the chemiluminescent emissions produced by various organometallic compounds passing through the reactive flow detector (RFD). The RFD spectra of osmium, rhenium and tungsten each display a broad continuum from approximately 400 to 800 nm, whose emitting species remain unidentified. The luminescence spectra of lead, chromium, ruthenium, iron and manganese in the reactive flow are each composed of both molecular emission bands, (e.g. metal oxide systems) and atomic emission lines. Compared with the chemiluminescent spectra obtained for these elements in the flame photometric detector (FPD), the atomic emissions in the RFD are relatively more abundant and more intense than the molecular emissions. Additionally, the RFD produces lines of higher energy than the FPD. The highest atomic excitation energy observed in the reactive flow is that of the 280-nm manganese lines (approximately 4.4 eV). This apparent 'energy limit' is in excellent agreement with the energy produced by the recombination of hydrogen radicals (4.5 eV), thus implying that this reaction may be the primary source of excitation energy in the reactive flow. © 2002 Elsevier Science B.V. All rights reserved.

**Keywords:** Reactive flow; Chemiluminescence; Organometallic compounds; Spectra; Excitation energy

## 1. Introduction

A wide variety of molecular emission devices are used as detectors in chromatography, owing to the selectivity and sensitivity they provide to various hetero-atomic compounds [1–4]. Among these devices, monitors of chemiluminescence are often employed in the selective detection of certain

elements such as sulfur [5–7] and nitrogen [8,9]. One of the most widely used chemiluminescent sensors is the flame photometric detector (FPD) [2–4,10–12].

Although the FPD is primarily known as a relatively inexpensive, reliable detector for determining organic compounds containing sulfur, phosphorus or tin [13–15], it also yields sensitive and selective responses towards iron, manganese, ruthenium, chromium and many other elements [16–21]. While molecular emission usually domi-

\*Corresponding author. Tel.: +1-403-220-5370; fax: +1-403-289-9488.

E-mail address: thurbide@ucalgary.ca (K.B. Thurbide).

nates FPD spectra, some low-energy atomic emissions (most often resonance lines) have also been observed for several metals in this detector [16–20]. These lines were obtained from a typical FPD, possessing a hydrogen-rich flame of relatively low temperature. In contrast to the thermal excitation typical of conventional atomic spectroscopy, the FPD relies on chemiluminescent excitation to produce atomic emissions.

A few years ago we introduced a new type of hydrogen-rich chemiluminescent sensor called the ‘reactive flow detector’ (RFD) [22]. The RFD monitors emissions from the luminescent column of a hydrogen/air pre-mixture, which is in the process of reacting while flowing through a glass or quartz capillary. The RFD offers sensitive and selective responses towards volatile sulfur, phosphorus and tin containing compounds [22,23]. Its optical emissions are spectrally similar to those of the common FPD.

For instance, the primary sulfur emitter in both detectors is  $S_2^*$ . Either device can also provide linear sulfur response by monitoring  $HSO^*$  at 750 nm [22]. Similarly, both detectors produce phosphorus emission in the form of HPO bands. Furthermore, both offer tin emission: either from the quartz surface (emitter unknown) or, less sensitively, from the gas phase ( $SnH^*$ ). As well, the faint background emission in the RFD and the FPD consist predominantly of OH bands. In accordance with these spectral features, the analytical sensitivity and selectivity towards sulfur, phosphorus and tin are similar among the two detectors.

On the other hand, there also exist substantial differences between the RFD and the FPD. Most notably, the RFD does not exhibit analyte response quenching in the presence of hydrocarbons [24] (which is a common interference that seriously hampers the FPD analysis of complex matrices [25]). Furthermore, the FPD is known to produce different emission spectra for aliphatic ( $CH^*$ ) and aromatic ( $CH^*$  and  $C_2^*$ ) hydrocarbons, and is more sensitive towards the latter [20]. In contrast, the RFD produces  $CH^*$  exclusively for both and responds equally to either [22]. These findings indicate a significant difference between the RFD and the FPD in their respective chemistries of

degrading hydrocarbons and/or promoting analyte emissions.

In order to gain more knowledge of the chemistry through which the reactive flow operates, further investigation of the RFD was needed. Given both similarities and differences between the RFD and the FPD, it seemed appropriate to examine the spectra of more elements in the reactive flow, in order to compare any observed emission with documented FPD spectra and other available data. Since the FPD has been studied for over three decades, many of its analytical and chemical properties have been established, and it therefore provides a most useful system of reference. In particular, a comparison of RFD and FPD emission spectra may reveal information about the energy transfer and excitation mechanism(s) within the reactive flow. This paper will report the RFD emission spectra of several metals, particularly those that are known to produce a wider variety of chemiluminescent continua, molecular emission bands and/or atomic emission lines in the FPD. A discussion of the major spectral features and, where possible, the identification of species emitting in the RFD will be presented in an effort to learn more about the chemistry within this unique new source of chemiluminescence.

## 2. Experimental

A detailed description of the RFD has been previously given [22]. Briefly, the detector is constructed on the base of an old Tracor model 550 FID. The RFD creates a stable, luminescent gas column ( $\sim 35$  mm in length) by the low-temperature reaction of a fuel-rich hydrogen/air pre-mixture that flows, together with the column effluent, through a quartz or borosilicate glass capillary (35 mm  $\times$  1.8 mm I.D.). The emission is sampled midway down the capillary via a glass image conduit (6  $\times$  0.25 in O.D.; #38307, Edmund Scientific, Barrington, NJ, USA) or a quartz rod that guides the light to a photomultiplier tube (PMT) (R-374 or R-1104 with wavelength range of 185–850 nm; Hamamatsu, Bridgewater, NJ, USA). Two or more orthogonal channels can be similarly operated by monitoring the same area of the reactive flow through another light guide/PMT

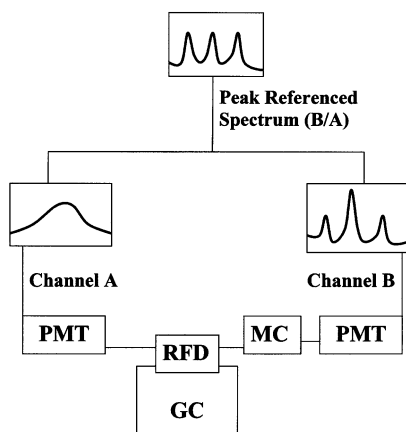


Fig. 1. Schematic representation of the instrumental arrangement used to collect a typical peak referenced spectrum. The individual components shown in the figure are a gas chromatograph (GC), a reactive flow detector (RFD), a monochromator (MC) and photomultiplier tubes (PMT).

configuration. Spectra are acquired by placing a 1/4 m Jarrell–Ash monochromator (1180 lines/mm grating, 3 nm/mm bandpass) or an Oriol model 77250 1/8 m monochromator (#77298 grating; 1200 lines/mm, 6 nm/mm bandpass) between the light guide and the PMT.

Spectra are recorded using a two-channel ‘single-peak’ method developed earlier by our group for concentration-referenced, on-line spectral scanning of migrating GC peaks [26]. This method is based on scanning the spectral chemiluminescence of a single chromatographic peak during its passage through the RFD system, as shown in Fig. 1. In this dual-channel configuration, the non-dispersive channel (channel A in Fig. 1) records the chromatographic signal profile, while the other, wavelength dispersive channel (channel B in Fig. 1) scans the emission spectrum. The signal from the dispersive channel is then divided by the signal from the non-dispersive channel for each unit of optical sampling time, in order to obtain the final, ‘peak referenced’ spectrum with the correct intensity distribution. The wavelength indicator on the monochromator is calibrated using mercury lines as a standard. A borosilicate column (2 m × 1.8 mm I.D.) packed with 10% Apiezon L on Chromosorb W (45–60 mesh) is used to perform gas-

chromatographic separations. Typical gas flows are 12 ml/min nitrogen through the column, 40 ml/min hydrogen and 60 ml/min air through the reactive flow capillary, and 150 ml/min air through the detector housing. All other conditions are outlined in the text.

### 3. Results and discussion

The elements investigated in this study include chromium, lead, ruthenium, iron, manganese, rhenium, osmium and tungsten. While analytical interests in these elements vary, they were chosen primarily for their wide range of spectral features and response characteristics in the FPD, in the expectation that they would yield similar emissions in the RFD. The luminescence spectrum for each metal in the RFD was extensively scanned, involving several trials and covering different wavelength regions, in order to verify the major features of observed emissions.

#### 3.1. Chromium

Fig. 2 shows the typical emission spectrum for chromium introduced to the RFD as chromium hexacarbonyl. The main spectral features were found to occur between 350 and 750 nm. Above

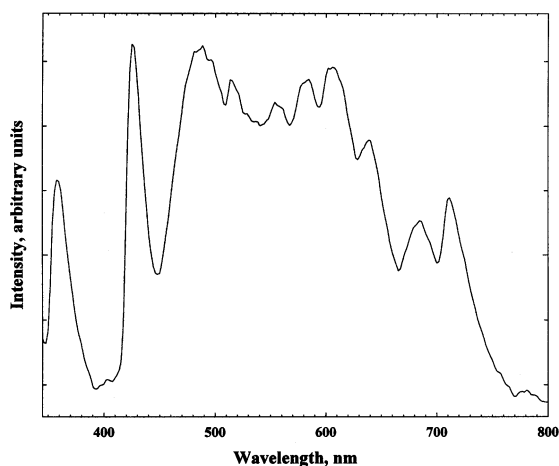


Fig. 2. Spectrum from chromium hexacarbonyl in the RFD; PMT: R-374, 1/4 m monochromator, nominal bandpass: 3 nm, scan: signal observed for a portion of a 20- $\mu$ g peak.

450 nm, a broad emission system abounds with band heads near 555, 580, 605, 640 and 685 nm. These bands agree very well with those attributed to CrO [27,28]. Additionally, there are two major features centered at approximately 425 and 357 nm (the latter is also seen in second order near 714 nm). These emissions are broader than the optical bandwidth (3 nm), and are situated where clusters of prominent atomic lines have been reported for chromium near 357, 359, 360, 425, 427 and 428 nm [28–30]. In all, the RFD spectrum for chromium is very similar to that produced by chromium in the FPD [20]. However, the intensity of the atomic lines for chromium, relative to the CrO molecular bands, is larger in the RFD than it is in the FPD. Furthermore, lines of higher energy are comparatively favored. This is particularly noticeable in Fig. 2 for the composite of chromium emission lines near 357 nm, which are of comparable intensity to the atomic emissions near 425 nm and the CrO band system, whereas in the FPD they are much smaller [20]. Another difference involves the atomic emission of chromium near 520 nm [29,30]. Although the use of this wavelength for monitoring chromium by FPD has been reported [31], the 520-nm atomic chromium emission was not observed in subsequent hydrogen-rich and stoichiometric flame comparisons of the FPD [20]. As seen in Fig. 2, the RFD spectrum displays an emission at 520 nm that appears to correspond to this composite of atomic lines for chromium.

### 3.2. Lead

The RFD spectrum for lead, as obtained from tetraethyl lead, is shown in Fig. 3. It consists predominantly of a red degraded band system between 350 and 600 nm. Superimposed on this system are two major features that correlate well with intense atomic emission lines known from the literature near 364, 368 and 406 nm [28–30]. These lines originate from upper states at 35 287, 34 960 and 35 287  $\text{cm}^{-1}$ , respectively, and are not resonance lines. The 35 287  $\text{cm}^{-1}$  state also gives rise to the less intense 283-nm resonance line, which was not observed in the RFD, as discussed later in the text. A noticeable series of smaller

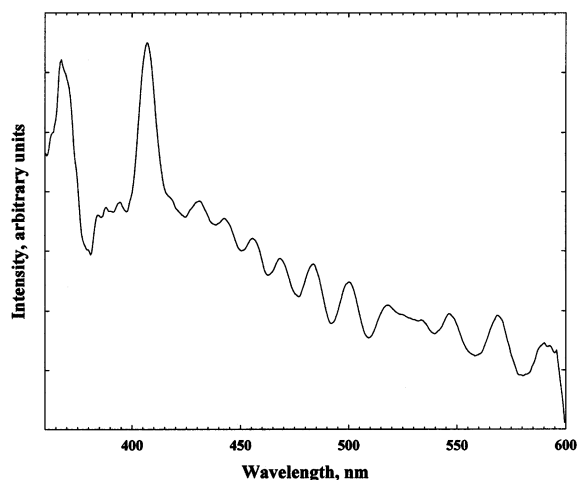


Fig. 3. Spectrum from tetraethyl lead in the RFD; PMT: R-1104, 1/8 m monochromator, nominal bandpass: 6 nm, scan: signal observed for a portion of a 20- $\mu\text{g}$  peak.

band heads on the system are located approximately 431, 441, 455, 466, 482, 498, 516, 535, 546, 568 and 591 nm. This series matches very well the emission spectrum of PbO [27]. Although the chemiluminescence spectrum for lead in the FPD has been reported, the low light levels and the filter monochromator used in the original study prevented the absolute assignment of emissive species potentially linked to PbO [21]. A later study of lead response, using a wide variety of flow conditions in the 'holophotal' FPD, demonstrated the likely presence of at least three different spectral features by principal component analysis. Although the excited species were again not identified, the FPD spectrum taken at near stoichiometric conditions clearly shows the PbO bands mentioned above [32]. Similarly, the RFD spectrum for lead reveals the PbO band system, although the prominent atomic emissions seen for lead in the RFD were not mentioned in the FPD literature [21,32].

### 3.3. Ruthenium

Fig. 4 displays the RFD emission spectrum for ruthenium, introduced as ruthenocene, between 340 and 540 nm. There appear some major features near 342, 344, 350, 373 and 380 nm, which

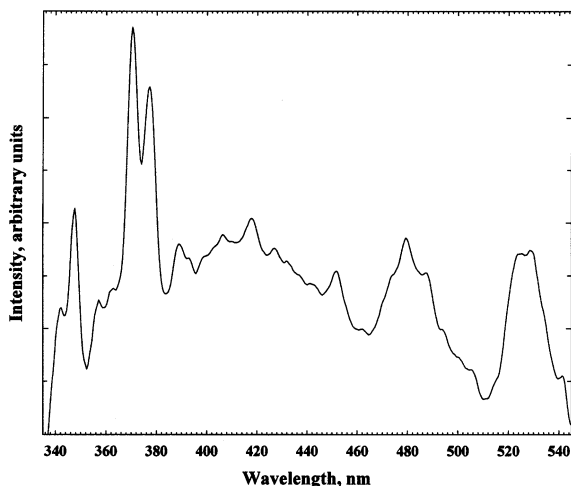


Fig. 4. Spectrum from ruthenocene in the RFD; PMT: R-1104, 1/8 m monochromator, nominal bandpass: 3 nm, scan: signal observed for a portion of a 1- $\mu$ g peak.

correspond to the wavelengths of prominent atomic emission lines [28–30]. Additionally, less intense lines may be present near 392, 421 and 455 nm, the latter of which would have to come from an upper state at 28 495  $\text{cm}^{-1}$ . In all, the spectrum resembles quite closely that of ruthenocene in the FPD [18]. It includes the appearance of two broad features near 484 and 528 nm, the emitting species for which has not been identified but could possibly have been RuH [18]. A notable difference between the RFD and FPD spectra for ruthenium, however, is the relative intensity of the major spectral features. While the FPD displays, almost entirely, the unassigned spectral features at 484 and 528 nm, the RFD spectrum for ruthenium is dominated by the presence of atomic emission lines.

### 3.4. Iron

The emission spectrum for iron introduced as ferrocene into the RFD is shown in Fig. 5. Very similar to the FPD [16,26], the RFD shows a spectrum for iron with major features near 344, 372 and 385 nm, which correlate with prominent atomic emission lines for iron. As well, a much less intense series of emission bands above 400

nm has already been seen in the FPD iron spectrum. It is of unknown origin, but may be related to FeO [16]. While these features, and their respective intensities, otherwise agree very closely between RFD and FPD, one feature in the RFD spectrum of ferrocene was absent in the FPD. To wit, a moderately intense peak centered near 302 nm appears in the RFD spectrum of iron, which displays finer structural features when retraced at one-half the optical bandpass. These features correlate with a cluster of atomic lines (mostly of the resonance type) that are known to occur in this region between approximately 296 and 306 nm. The most prominent of these lines is located near 302 nm [28–30].

### 3.5. Manganese

Manganese was introduced to the RFD as methylcyclopentadienyl manganese tricarbonyl (MMT) and the resulting luminescence spectrum is displayed in Fig. 6. As can be seen, the spectrum consists almost exclusively of a strong emission at 403 nm, corresponding to three closely spaced, prominent atomic emission lines for manganese [28–30]. Also present in Fig. 6 are contributions from a band system with features near 540, 560, 585 and 600 nm. This spectrum is similar to one

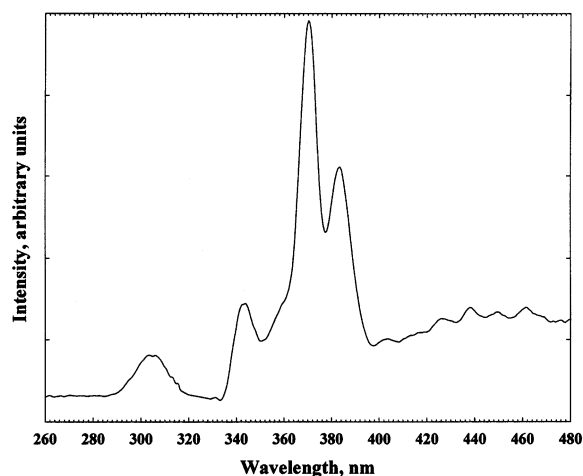


Fig. 5. Spectrum from ferrocene in the RFD, PMT: R-1104, 1/8 m monochromator, nominal bandpass: 6 nm, scan: signal observed for a portion of a 1- $\mu$ g peak.

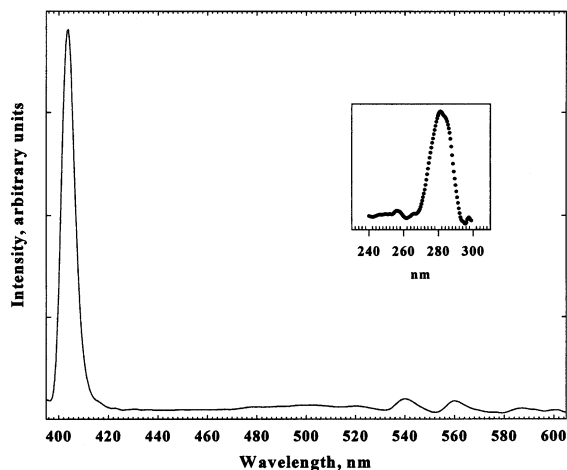


Fig. 6. Spectrum from MMT in the RFD, PMT: R-1104, 1/8 m monochromator, nominal bandpass: 3 nm, scan: signal observed for a portion of a 3- $\mu$ g peak.

produced from manganese in the FPD [17], except that the luminescence at 540 nm is much more intense in the FPD and has been described as possibly due to atomic emission. While this may also be true for the RFD, the distribution and the relative intensity of the band system correlates very well with the emission spectrum of MnO [27] upon closer inspection. Furthermore, it is much less intense, relative to the atomic 403-nm emission, when compared with the FPD spectrum. Of still greater interest, spectral scans below 300 nm reveal an emission at 280 nm, present at about the same intensity as that of the MnO system (Fig. 6 inset, expanded view). This feature corresponds to three prominent resonance lines of manganese that had not been observed in FPD spectra [17,28–30].

### 3.6. Rhenium, osmium and tungsten

Although most of the RFD spectra for the investigated metals appeared to be composed of characteristic atomic emission lines and molecular emission bands, this was not the case for certain other elements. Fig. 7 displays the spectra typically obtained for rhenium (introduced as di-rhenium decarbonyl), osmium (osmocene) and tungsten (tungsten hexacarbonyl) in the RFD. By comparison, these spectra have no distinguishable features

other than a broad continuum spanning the region from approximately 400 to 800 nm, which did not display any finer structural features when examined with a narrower optical bandpath. At present, the emitting species for these spectra, which agree well with corresponding spectra from the FPD [19,20,33], are unknown. While an exact correlation with literature spectra could not be established, similar continua in the FPD have been postulated to arise from emissions of polyatomic aggregates [20]. Although this is only speculative, it is interesting to note that molecules such as di- and tri-oxide complexes of rhenium and osmium have been observed to yield a broad luminescence in the 600–900 nm region [34].

As in the earlier case of the FPD, the assertion that atomic emission lines are present in many of

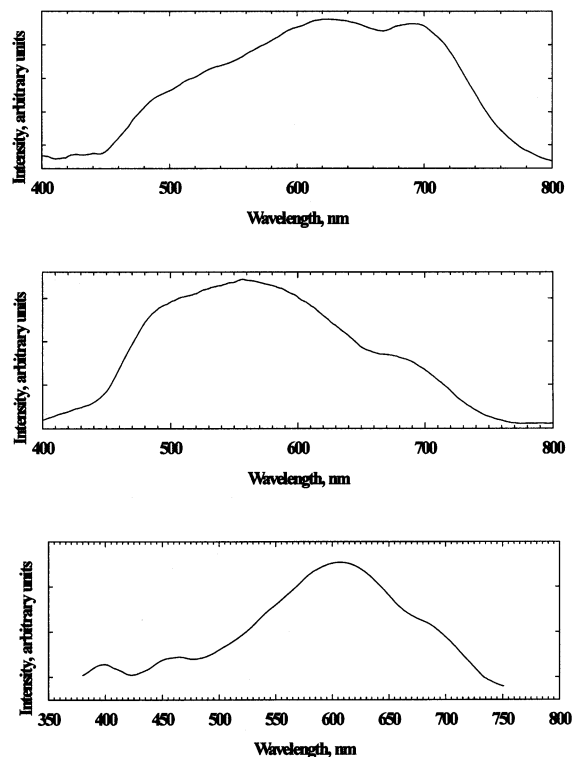
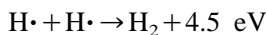


Fig. 7. Spectrum from di-rhenium decarbonyl (upper trace), osmocene (middle trace) and tungsten hexacarbonyl (lower trace) in the RFD, PMT: R-374, 1/4 m monochromator, nominal bandpass: 30 nm, scans: signal observed for a portion of a 5- $\mu$ g peak.

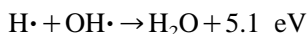
the RFD spectra is based primarily on the agreement of experimentally observed emission wavelengths with prominent spectral literature values. Where possible, the investigation of finer structural features within these emissions has been pursued. However, in both RFD and FPD, measurements at very high resolution are typically not possible because of the low (absolute) emission intensities. For example, the three atomic lines present in the 403-nm manganese emission are located approximately 0.2 nm from each other. By way of comparison, the best resolution ever obtained for atomic lines (of iron in this case) in the FPD was limited to a bandpass of approximately 1 nm [26]. It is interesting to note, however, that when using a broader bandpass of approximately 5 nm, this same emission very closely resembles the composite atomic lines seen in the iron spectrum of Fig. 5. It should also be mentioned that, although both RFD and FPD were run at optimized conditions for acquiring spectra, the ‘optimization’ was not of the same kind. In the RFD, the stability of the reactive flow dictates, to a large extent, the flow settings. In the FPD, a much wider range of flow conditions is available for obtaining the largest signal/noise ratio. In any case, a closer examination of the reactive flow, in regard to the energy that it provides as a spectral excitation source, would certainly be helpful.

Similar to the FPD, the RFD also derives its excitation energy from chemiluminescence. While this is fairly obvious from such basic observations as its low temperature ( $\sim 230$  °C), it is also supported by the fact that certain elements give rise to a large response in the RFD, while others are not recognized at all, (e.g. vanadium, magnesium and aluminum). This indicates that emission in the reactive flow cannot be simply due to a thermal excitation process. Thus, if chemiluminescence is the primary source of excitation in the reactive flow, it would be of interest to know how much energy it affords the RFD and from which chemical processes.

According to a theory preceding the FPD, but used on various occasions to explain its mode of operation, chemiluminescent energy is often obtained from the recombination of hydrogen radicals [35]



and/or the formation of water [35]



Spectral studies have indicated that the largest excitation energy observed so far in the FPD was approximately 3.6 eV ([20], cf. [26]). While the hydrogen recombination mechanism could more than provide that energy, the apparent presence of an experimental 3.6 eV ‘limit’ raises the question of whether hydrogen recombination does indeed play the assumed dominant role in the FPD. However, given the variety of flame parameters possible with that device [32,33], continued investigations using analytically and/or spectrally optimized FPD conditions may still produce a larger energy ‘limit’. On the other hand, lower energy routes such as analyte excitation via metal hydrides cannot be excluded either [20].

By comparison, the RFD spectra clearly extend beyond this apparent FPD energy limit. For instance, the cluster of Fe lines near 302 nm ( $\sim 4.1$  eV) supplies evidence for an excitation energy larger than 3.6 eV. Of the RFD spectra recorded, the manganese lines near 280 nm ( $\sim 4.4$  eV) mark the highest excitation energy observed. While other UV regions were scanned for prominent emissions, such as the atomic iron lines near 271 nm ( $\sim 4.6$  eV) and manganese lines near 260 nm ( $\sim 4.8$  eV), none of these were observed. Thus, 4.4 eV may well represent the ‘energy limit’ of the RFD. This is in very good agreement with the energy provided by the recombination of hydrogen radicals (4.5 eV). It indicates that this flame reaction could be the predominant mode of chemical excitation in the RFD. Similar to the FPD, however, this apparent limit does not account for the absence of other prominent atomic emissions within this energy range, such as the lead resonance line at 283 nm (4.3 eV). Likewise, other elements such as rhenium, osmium and tungsten, while emitting broad continua, emit none of the prominent atomic emissions known to occur within this energy range.

Still, an apparent limit in energy of the reactive flow does not necessarily imply that a single reaction is equally responsible for the excitation of all elements. The variety of molecular emissions

observed in the RFD and the very nature of chemiluminescence, suggests that excitation, or lack thereof, depends less on the energy of the excited state than on the nature of the element involved. In this regard, it is interesting to note that the 283-nm resonance line for lead mentioned above is of prominent intensity in high energy arc/spark sources [29,30]. However, in studies using an oxygen/acetylene and an air/hydrogen flame source, the same line was not observed relative to an intense 406-nm lead line [28]. Furthermore, when using an oxygen/hydrogen flame source, the 283-nm lead line was present at an intensity almost two orders less than that of the 406-nm line, even though both atomic emissions arise from the same excited state [28]. Other compilations report as well that the 283-nm lead line was not observed in such flame sources, but that the 406-nm line was very intense [36]. Thus, clearly, if a fast chemical channel is available for molecular or continuum emission (or for a non-luminescent reaction), the atomic emission, while energetically possible, may not be seen. Still, wherever atomic lines have been observed in reactive-flow spectra, approximately 4.4 eV does indeed appear to be the largest amount of excitation energy available.

The proposition that hydrogen radical recombination is one of the dominant excitation reactions in the reactive flow is obviously supported by the high concentration of hydrogen radicals in this system and certainly agrees with the hydrogen-rich nature of the RFD, as well as with other observations. For example, the surprising fact that hydrocarbons do not quench chemiluminescent emissions in the RFD has been previously linked to the relative dearth of free oxygen atoms in the reactive flow as compared to the photometric flame [24,37]. As well, the slow combustion observed in the reactive flow has been speculated to propagate via peroxidic radicals, similar to the chemistry between the second and third explosion limits of the hydrogen/oxygen flame reaction [24,37]. While these hypotheses do not exclude the presence of oxygen atoms and other flame radicals in the RFD, they may explain why atomic lines are so prevalent, and so intense relative to metal oxide emissions, when compared to the same features

from the FPD. A higher concentration of hydrogen and a lower concentration of oxygen atoms should indeed produce this very effect.

This effect does not, however, demand that the reaction of hydrogen atoms with hydroxyl radicals, (i.e. 'water formation') be absent in the reactive flow. In fact, spectral evidence clearly shows  $\text{OH}^*$  to constitute almost exclusively the background of the RFD [24]. However, if the 'water formation' reaction were to cause significant analyte excitation in reactive flows (and typical FPD flames), it would be of interest to know why atomic lines of higher energy (up to 5.1 eV) have not been observed. Of further interest would be to know whether the metal oxide emission bands observed for several of the metals in this study originate from a direct reaction with oxygen atoms or from some other process involving hydroxide or peroxide radicals. While the present findings strongly indicate hydrogen recombination to be the primary source of excitation energy in the reactive flow, further studies are required to establish whether and to what extent other reactions contribute to analyte emission in the RFD.

#### 4. Conclusions

Several metals were observed to yield characteristic chemiluminescent emissions in the RFD. While many spectral features of the metal emissions were similar to those obtained in the FPD, the RFD showed a much larger ratio of atomic emission lines to molecular emission bands than the FPD. As with the FPD, the RFD produced only broad continua for rhenium, osmium and tungsten.

Some of the prominent atomic emissions displayed by elements such as iron, (e.g. a cluster of lines near 302 nm) and manganese (e.g. the 280-nm triplet) demonstrate that the RFD has a larger 'energy limit' (4.4 eV) than that reported thus far for the FPD (3.6 eV). The RFD energy limit is in excellent agreement with the energy supplied by hydrogen radical recombination (4.5 eV). The spectral data support the notion that this reaction may be the major source of chemiluminescent excitation energy in the RFD. The relative intensity of atomic emission lines compared to metal oxide

emission bands also supports the earlier postulated dearth of free oxygen atoms within the reactive flow. Further studies are needed, however, to verify the extent to which other reactions may contribute to reactive-flow excitation and to assess the analytical potential of these metal emissions in the RFD.

## Acknowledgments

This project was supported by an NSERC operating grant.

## References

- [1] J.C.T. Eijkel, H. Stoeri, A. Manz, A molecular emission detector on a chip employing a direct current microplasma, *Anal. Chem.* 71 (1999) 2600–2606.
- [2] G.A. Eiceman, H.H. Hill, J. Gardea-Torresdey, *Gas Chromatography*, *Anal. Chem.* 70 (1998) 321–340.
- [3] G.A. Eiceman, H.H. Hill, J. Gardea-Torresdey, *Gas Chromatography*, *Anal. Chem.* 68 (1996) 291–308.
- [4] G.A. Eiceman, H.H. Hill, J. Gardea-Torresdey, *Gas Chromatography*, *Anal. Chem.* 72 (2000) 137–144.
- [5] Y.C. Chen, J.G. Lo, Gas chromatography with flame ionization and flameless sulfur chemiluminescence detectors in series for dual channel detection of sulfur compounds, *Chromatographia* 43 (1996) 522–526.
- [6] T.C. Chasten, G.M. Silver, J.W. Birks, R. Fall, Fluorine induced chemiluminescence detection of biologically methylated tellurium, selenium, and sulfur compounds, *Chromatographia* 30 (1990) 181–185.
- [7] H. Wang, Q. Zhang, I.G. Dallahama, K.T. Chang, Analysis of both sulfur and non-sulfur compounds using a single gas chromatograph with parallel sulfur chemiluminescence and thermal conductivity detectors, *J. Chromatogr. Sci.* 36 (1998) 605–611.
- [8] A.D. Sokolowski, G. Vigh, Coupling of a gas-phase chemiluminescence nitrogen detector and a capillary electrophoretic system, *Anal. Chem.* 71 (1999) 5253–5257.
- [9] C.A. Lucy, C.R. Harrison, Chemiluminescence nitrogen detection in ion chromatography for the determination of nitrogen-containing anions, *J. Chromatogr.* 920 (2001) 135–142.
- [10] H. Singh, C.G. Eisner, W.A. Aue, Dual channel flame photometric detector for sensitive spectrum acquisition and variable wavelength operation, *J. Chromatogr.* 734 (1996) 405–409.
- [11] H.P. Tuan, H.G.M. Janssen, C.A. Cramers, E.M. Kuiper-van Loo, H. Vlap, Evaluation of the performance of various universal and selective detectors for sulfur determination in natural gas, *J. High Resol. Chromatogr.* 18 (1995) 333–342.
- [12] W. Wardencki, B. Zygmunt, Gas chromatographic sulphur sensitive detectors in environmental analysis, *Anal. Chim. Acta* 255 (1991) 1–13.
- [13] R.S. Hutte, J.D. Ray, Sulfur selective detectors, in: H.H. Hill, D.G. McMinn (Eds.), *Detectors for Capillary Chromatography*, John Wiley and Sons, Inc, New York, 1992, p. 193, Chapter 9.
- [14] S.S. Brody, J.E. Chaney, Flame Photometric Detector, *J. Gas Chromatogr.* 4 (1966) 42–46.
- [15] C.G. Flinn, W.A. Aue, Surface luminescence in the detection of organotin compounds following gas chromatography, *Can. J. Spectrosc.* 25 (1980) 141–148.
- [16] X.-Y. Sun, W.A. Aue, Selective detection of volatile iron compounds by flame photometry, *J. Chromatogr.* 467 (1989) 75–84.
- [17] W.A. Aue, B. Millier, X.-Y. Sun, Determination of (methycyclopentadienyl) manganese tricarbonyl in gasolines by gas chromatography with flame photometric detection, *Anal. Chem.* 62 (1990) 2453–2457.
- [18] X.-Y. Sun, W.A. Aue, Detection at the picogram level of bis(cyclopentadienyl) ruthenium by gas chromatography-flame photometry, *Can. J. Chem.* 67 (1989) 897–901.
- [19] X.-Y. Sun, W.A. Aue, Detection of osmocene by gas chromatography-flame photometry, *Mikrochim. Acta* 1 (1990) 1–6.
- [20] X.-Y. Sun, B. Millier, W.A. Aue, Flame photometric detection of some transition metals. I: Calibrations and spectra. II: Enhancement of selectivity, *Can. J. Chem.* 70 (1992) 1129–1142.
- [21] W.A. Aue, X.-Y. Sun, B. Millier, Inter-elemental selectivity, spectra and computer-generated specificity of some main group elements in the flame photometric detector, *J. Chromatogr.* 606 (1992) 73–86.
- [22] K.B. Thurbide, W.A. Aue, Reactive-flow luminescence detector for gas chromatography, *J. Chromatogr.* 684 (1994) 259–268.
- [23] K.B. Thurbide, W.A. Aue, Analysis of organotin compounds by gas chromatography reactive flow detection, *J. Chromatogr.* 858 (1999) 245–250.
- [24] K.B. Thurbide, W.A. Aue, Quenching-free reactive-flow photometry, *J. Chromatogr.* 694 (1995) 433–440.
- [25] K.B. Thurbide, W.A. Aue, High-throughput reactor for simulating the flame photometric detector, *J. Chromatogr.* 905 (2001) 241–250.
- [26] H. Singh, W.A. Aue, Accurate spectral scans of single chromatographic peaks, *J. Chromatogr.* 746 (1996) 43–51.
- [27] P.W.B. Pearse, A.G. Gaydon, *The Identification of Molecular Spectra*, 4th edition, Chapman and Hall, London, 1976.
- [28] M.L. Parsons, P.M. McElfresh, *Flame Spectroscopy: Atlas of Spectral Lines*, 1st edition, Plenum, New York, 1971.

- [29] A.N. Zaidel, V.K. Prokof'ev, S.M. Raiskii, V.A. Slavnyi, E.Ya. Shreider, *Tables of Spectral Lines*, 3rd edition, Plenum, New York, 1970.
- [30] W.F. Meggers, C.H. Corliss, B.F. Scribner, *Tables of Spectral Line Intensities*, 1st edition, NBS Monograph 32, U.S. Government, Washington DC, 1961.
- [31] C.A. Burgett, L.E. Green, 'An improved flame photometric detector for gas chromatography', *Spectrochim. Acta Part B* 30 (1975) 55–60.
- [32] J.A. Gebhardt, Master's Thesis, Dalhousie University, Halifax, Nova Scotia, 1994.
- [33] N.B. Lowery, PhD Thesis, Dalhousie University, Halifax, Nova Scotia, 1995.
- [34] C. Savoie, C. Reber, Coupled electronic states in trans-dioxo complexes of rhenium(V) and osmium(VI) probed by near-infrared and visible luminescence spectroscopy, *J. Am. Chem. Soc.* 122 (2000) 844–852.
- [35] T.M. Sugden, A.M. Demerdache, Emission spectra of sulphur, *Nature* 195 (1962) 596.
- [36] M.L. Parsons, B.W. Smith, G.E. Bentley, *Handbook of Flame Spectroscopy*, Plenum, 1st edition, New York, 1975.
- [37] W.A. Aue, K.B. Thurbide, Reactive-flow luminescence with flame ionization detection, *J. Chromatogr.* 699 (1995) 183–193.